

Reexamination of the standard model nucleon electric dipole moment

Chien-Yeah Seng

Amherst Center for Fundamental Interactions, Department of Physics, University of Massachusetts - Amherst, Amherst, Massachusetts 01003, USA

(Received 17 November 2014; revised manuscript received 19 January 2015; published 13 February 2015)

The Cabibbo-Kobayashi-Maskawa matrix in the standard model is currently the only experimentally confirmed source of CP violation. The intrinsic electric dipole moment of the nucleon induced by this CP phase via hadronic loop and pole diagrams was studied more than two decades ago, but is subject to various theoretical issues such as the breakdown of chiral power counting and uncertainties in the determination of low energy constants. I carry out an up-to-date re-analysis on both one-loop and pole diagram contributions to the nucleon electric dipole moment based on heavy baryon chiral perturbation theory in a way that preserves power counting, and I redo the determination of the low-energy constants following the results of more recent articles. Combined with an estimation of higher-order contributions, I expect the long-distance contribution to the standard model nucleon electric dipole moment to be approximately $(1 \times 10^{-32} - 6 \times 10^{-32}) e \text{ cm}$.

DOI: [10.1103/PhysRevC.91.025502](https://doi.org/10.1103/PhysRevC.91.025502)

PACS number(s): 13.40.Em, 12.39.Fe

I. INTRODUCTION

The search for the permanent electric dipole moment (EDM) of elementary and composite particles is motivated by its CP violating nature. We live in a universe in which the amounts of baryons and antibaryons are unequal. In order to explain this asymmetry, CP-violating interactions are needed to fulfill one of the three Sakharov criteria [1]. EDMs of elementary and composite particles are, in most cases, direct consequences of these interactions which can be probed in low-energy experiments. Since the first upper limit on the neutron EDM obtained by Smith, Purcell, and Ramsey in 1957 [2], numerous experiments have been performed to improve the sensitivity of EDM measurements in different particle systems. Currently, the most stringent bounds on EDMs are set for the electron ($8.7 \times 10^{-29} e \text{ cm}$, 90% C.L.) [3] and the mercury atom ($3.1 \times 10^{-29} e \text{ cm}$, 95% C.L.) [4], while the current upper limits on neutron and proton EDMs are $2.9 \times 10^{-26} e \text{ cm}$ (90% C.L.) [5] and $7.9 \times 10^{-25} e \text{ cm}$ (95% C.L.) respectively (the latter is deduced from the bound on the mercury EDM). Future experiments are designed (or have been considered) to push these bounds even further down. For the neutron EDM, this includes the experiment at Paul Scherrer Institut (PSI) [6], the CryoEDM and PNPI/ILL experiment at Institut Laue-Langevin (ILL) [7], the SNS neutron EDM experiment at Oak Ridge, the TRIUMF experiment in Canada, and the Munich experiment at Germany. These experiments are designed to reach a $10^{-28} e \text{ cm}$ precision level for the neutron EDM [8]. Also, both COSY [9] and BNL [10] have proposed storage ring experiments designed to measure the proton EDM to a level of $10^{-29} e \text{ cm}$ precision.

Although numerous beyond-standard-model (BSM) scenarios have been proposed that give rise to measurable EDMs within current experimental precision level, so far no definitive signal of such physics has been observed.¹ Therefore, the CP-violating phase of the Cabibbo-Kobayashi-Maskawa (CKM)

matrix in the standard model (SM) remains the only source for intrinsic EDMs. Questions have been raised concerning the expected size of EDMs coming from purely SM physics [11]. A simple dimensional analysis using constituent quark masses may suggest that the SM-induced neutron EDM could be as large as $10^{-29} e \text{ cm}$, approaching the level of sensitivity for future EDM experiments. It is therefore important to have a better estimate for the SM contribution to the nucleon EDM. To leading order, the quark EDM induced by the CKM matrix starts at three loops [12]. A detailed calculation showed that the valence-quark contribution to the neutron EDM is of order $10^{-34} e \text{ cm}$ [13]. It was also shown that long-distance contributions, namely contributions with baryons and mesons as effective degrees of freedom (DOFs), could generate a much larger hadronic EDM. For instance, the pion-loop contribution to the neutron EDM was first studied in a paper by Barton and White [14] which produced log-divergent results in the chiral limit, indicating that the long-range contribution may dominate. On the other hand, in a series of papers, Gavela *et al.* studied the pole-diagram contribution with the CP-violating phase generated by $|\Delta S| = 1$ electroweak [15] and gluonic penguin diagrams [16]. They claimed that the latter is dominant and derived a SM neutron EDM of order $10^{-31} e \text{ cm}$. The possibility of a long-range contribution to the neutron EDM from the CKM matrix was first pointed out by Khriplovich and Zhitnitsky [17]. He *et al.* [18] did a thorough chiral-loop calculation and re-analyzed the pole-diagram contribution in [15,16] and argued that the two are of the same order of magnitude. Their estimate for the neutron EDM is $1.6 \times 10^{-31} - 1.4 \times 10^{-33} e \text{ cm}$, which is currently the most widely accepted estimate for the SM neutron EDM. In recent years, the charm contribution to nucleon EDMs is also considered and it is roughly $10^{-31} e \text{ cm}$ [19].

The purpose of this paper is to revisit the previous study of both chiral-loop and the pole contributions to the nucleon EDM

¹There are indeed some hopeful candidates, for example the muon $g - 2$ anomaly; but no conclusive statement can be made before

one could further improve the experimental precision and reduce the theoretical uncertainty of the SM prediction.

in order to sharpen our SM benchmark value. On the theoretical side, one could improve earlier work in several ways. For instance, the chiral loop calculation in [18] adopted an older meson theory utilizing a pseudoscalar strong baryon-meson coupling that should be replaced by the standard axial-vector coupling. Also, their work that utilized an effective hadronic Lagrangian in computing chiral-loop diagrams faced another well known problem in the loss of power counting similar to that happening in the relativistic chiral perturbation theory (ChPT). ChPT is a nonrenormalizable theory that involves infinitely many interaction terms. Its predictive power therefore relies on the fact that higher-order terms are suppressed by powers of p/Λ_χ , where p is the typical mass or momentum scales of hadronic DOFs, and $\Lambda_\chi \sim 1$ GeV. This expansion, however, becomes ambiguous when baryons are included because a typical baryon mass is $M_B \sim 1$ GeV. Therefore, M_B/Λ_χ is no longer a small expansion parameter. Heavy baryon chiral perturbation theory (HBchPT) [20] provides a convincing way to get around this issue by performing a field redefinition in the baryon field to scale out its mass dependence. By doing this, one can split the baryon field into “light” and “heavy” components, where the former depends only on its residual momentum which is well below 1 GeV. After integrating out the heavy component of the baryon field, the effective Lagrangian can be written as a series expansion of $1/m_N$. This eliminates the possibility of a factor m_N appearing in the numerator and thus restores the power counting. Many works have appeared recently calculating the nucleon EDM induced by different BSM physics using HBchPT (see [21] for a general overview). Although the convergence of the SU(3) HBchPT is not as good as its SU(2) counterpart because m_K/m_N is not very small [22–26], it is still theoretically beneficial as it provides a formal classification of different contributions into leading and subleading orders. In this work, the chiral-loop contributions to the nucleon EDM are recalculated up to the leading order (LO) in the heavy baryon (HB) expansion.

Additionally, previous numerical results of loop and pole contributions face large uncertainties due to poorly known values of physical constants in the weak sector at that time. For example, the CP-violating phase δ of the CKM matrix quoted in Ref. [18] had an uncertainty that spans one order of magnitude. The fitting of certain low-energy constants (LECs), such as weak baryon-meson interaction strengths, has been updated since. Also, their theoretical estimation of various CP-phases in the effective weak Lagrangian was based on older work [27,28] which had been improved by others. Furthermore, for previous work on pole contributions, their estimation on effective CP phases was based only on a single gluonic penguin operator without considering the full analysis of operator mixing and renormalization group running. Moreover, the approximate form of their analytic expressions was based on the out-of-date assumption that $m_t \ll m_W$. In this work, I do a more careful determination of weak LECs, taking all these issues into account. Combining my calculation and an estimate of higher-order effects, I predict a range of the long-distance SM contribution to the nucleon EDM to be around $(1\text{--}6) \times 10^{-32}$ e cm. I identify the main sources of uncertainty and discuss possible steps

one could take to improve upon that. At the same time, I use dimensional analysis to estimate the size of possible short-distance counterterms. I find that they could be as large as 4×10^{-32} e cm.

This work is arranged as follows: in Sec. II, I will briefly outline the main ingredients of the SU(3) HBchPT and introduce the weak Lagrangian responsible for the generation of the nucleon EDM. In Sec. III, I will determine the LECs. In Secs. IV and V, I derive the analytic expressions for loop and pole contributions to the nucleon EDM respectively and calculate their numerical values. In Sec. VI, I will provide some further discussions and draw my conclusions.

II. HBchPT: STRONG AND ELECTROWEAK INTERACTIONS

In this section, I review some basic concepts of ChPT with the primary aim of establishing conventions and notation. ChPT is a low-energy effective field theory (EFT) of quantum chromodynamics (QCD) with hadrons as low-energy DOFs. QCD exhibits a global chiral symmetry in the limit of massless quarks. However, this symmetry is spontaneously broken in the ground state and leads to the emergence of Goldstone bosons which are identified as pseudoscalar mesons. The corresponding EFT obeys the same symmetry. An infinite tower of operators respecting the symmetry with increasing mass dimensions is organized in the Lagrangian. However, only a finite number of operators are retained since the dropped higher-dimensional operators make contributions that are suppressed by powers of p/Λ_χ .

I use the standard nonlinear representation of chiral fields [29–31], in which the pseudoscalar meson octet is incorporated in the exponential function $U = \exp\{i\phi/F_\pi\}$, where

$$\phi = \sum_{a=1}^8 \phi_a \lambda_a = \begin{pmatrix} \pi^0 + \frac{1}{\sqrt{3}}\eta_8 & \sqrt{2}\pi^+ & \sqrt{2}K^+ \\ \sqrt{2}\pi^- & -\pi^0 + \frac{1}{\sqrt{3}}\eta_8 & \sqrt{2}K^0 \\ \sqrt{2}K^- & \sqrt{2}\bar{K}^0 & -\frac{2}{3}\eta_8 \end{pmatrix} \quad (1)$$

with $F_\pi \approx 93$ MeV. The matrix U transforms under the chiral rotation as $U \rightarrow LUR^\dagger$, where L and R are elements of $SU(3)_L$ and $SU(3)_R$ respectively. The mass term of the meson octet is introduced using spurion analysis: the QCD Lagrangian would exhibit chiral invariance if the quark mass matrix $M = \text{diag}\{m_u, m_d, m_s\}$ transforms as $M \rightarrow LMR^\dagger$. Therefore, its low-energy effective theory written in terms of the spurion field M should also exhibit a similar invariance. The lowest-order operator that is invariant is $\text{Tr}[MU^\dagger + UM^\dagger]$. This operator gives rise to nonzero meson masses which are isospin symmetric.

The ground state $J^P = (1/2)^+$ baryon octet is assembled into the matrix

$$B = \begin{pmatrix} \frac{\Sigma^0}{\sqrt{2}} + \frac{\Lambda}{\sqrt{6}} & \Sigma^+ & p \\ \Sigma^- & -\frac{\Sigma^0}{\sqrt{2}} + \frac{\Lambda}{\sqrt{6}} & n \\ \Xi^- & \Xi^0 & -\frac{2\Lambda}{\sqrt{6}} \end{pmatrix}. \quad (2)$$

It transforms as $B \rightarrow K B K^\dagger$ with $K = K(L, R, U)$ being a unitary matrix. In order to couple baryons with the pseudoscalar octet, we define $\xi = \sqrt{U}$ which transforms as $\xi \rightarrow L \xi K^\dagger = K \xi R^\dagger$ and introduce the Hermitian axial vector

$$\mathcal{A}_\mu = \frac{i}{2} [\xi \partial_\mu \xi^\dagger - \xi^\dagger \partial_\mu \xi], \quad (3)$$

which transforms as $\mathcal{A}_\mu \rightarrow K \mathcal{A}_\mu K^\dagger$ under the chiral rotation (we have neglected its coupling with external fields because it is not needed in this work).

I now proceed with the formulation of HBchPT. In order to scale out the heavy mass-dependence, I rewrite its momentum as

$$p_\mu = m_N v_\mu + k_\mu, \quad (4)$$

where m_N is the nucleon mass, v_μ is the velocity of the baryon (which is conserved in the $m_N \rightarrow \infty$ limit) and k_μ is the residual momentum of the baryon which is well below 1 GeV. I therefore rescale the baryon field and retain its ‘‘light’’ component:²

$$B_v(x) = e^{i m_N v \cdot x} \frac{1 + \not{v}}{2} B(x). \quad (5)$$

The subscript v will be dropped from now on. I integrate out the remaining component which is ‘‘heavy.’’ The baryon propagator thus becomes

$$i S_B(k) = \frac{i}{v \cdot k - \delta_B + i\epsilon} \quad (6)$$

where $\delta_B = m_B - m_N$ is the baryon mass splitting. This procedure also reduces Dirac structures to either 1 or S^μ with the latter being the spin matrix of the baryon satisfying $S \cdot v = 0$. In this work I concentrate only on terms that are leading order in the HB expansion (with the exception of the baryon electromagnetic dipole transition operator that appears in pole diagrams, as I will explain below).

The lowest-order strong Lagrangian involving only the $(1/2)^+$ baryons, Goldstone bosons, and electromagnetic fields relevant to our work is given by

$$\begin{aligned} \mathcal{L} = & \frac{F^2}{4} \text{Tr}[\mathcal{D}_\mu U \mathcal{D}^\mu U^\dagger] + \frac{F^2}{4} \text{Tr}[\chi_+] + \text{Tr}[\bar{B} i v \cdot \mathcal{D} B] \\ & + 2D \text{Tr}[\bar{B} S^\mu \{A_\mu, B\}] + 2F \text{Tr}[\bar{B} S^\mu [A_\mu, B]] \\ & + \frac{b_D}{2B_0} \text{Tr}[\bar{B} \{\chi_+, B\}] + \frac{b_F}{2B_0} \text{Tr}[\bar{B} [\chi_+, B]] \\ & + \frac{b_0}{2B_0} \text{Tr}[\bar{B} B] \text{Tr}[\chi_+], \end{aligned} \quad (7)$$

where $D = 0.80$, $F = 0.50$ [29], and $\mathcal{D}_\mu U = \partial_\mu U + i e A_\mu [Q, U]$. Here $Q = \text{diag}\{2/3, -1/3, -1/3\}$ is the quark charge matrix while B_0 is a parameter characterizing the chiral quark condensate and $\chi_+ = 2B_0(\xi^\dagger M \xi^\dagger + \xi M \xi)$ introduces the quark-mass dependence. The last three terms in Eq. (7) are responsible for the mass splitting within the baryon octet [32]. Since I have scaled out the nucleon mass from the baryon field

B , the proton and neutron will appear as massless excitations and the other baryons will have an excitation energy given by the ‘‘residual’’ mass δ_B . This is important later during the computation of pole diagrams.

For the purpose of pole diagram contributions I need also to include the $(1/2)^-$ baryon octet. The importance of these resonances can be traced back to the observation of the unexpectedly large violation of Hara’s theorem [33] which states that the parity-violating radiative $B \rightarrow B' \gamma$ transition amplitude should vanish in the exact SU(3) limit. The authors of Ref. [34] (later improved by [35]) pointed out that this apparent puzzle could be resolved by including baryon resonances that give rise to pole diagrams which enhance the violation of Hara’s theorem. Therefore, one should naturally expect that the same kind of diagrams will also play an important role in the determination of the nucleon EDM. The resonance $(1/2)^-$ octet is denoted as \mathcal{R} :

$$\mathcal{R} = \begin{pmatrix} \frac{\Sigma^{0*}}{\sqrt{2}} + \frac{\Lambda^*}{\sqrt{6}} & \Sigma^{+*} & p^* \\ \Sigma^{-*} & -\frac{\Sigma^{0*}}{\sqrt{2}} + \frac{\Lambda^*}{\sqrt{6}} & n^* \\ \Xi^{-*} & \Xi^{0*} & -\frac{2\Lambda^*}{\sqrt{6}} \end{pmatrix}. \quad (8)$$

It transforms in the same way as B except that it has a negative intrinsic parity.

The part of strong and electromagnetic chiral Lagrangian involving \mathcal{R} which is relevant to our work is given by

$$\begin{aligned} \mathcal{L}_\mathcal{R} = & \text{Tr}[\bar{\mathcal{R}} i v \cdot \mathcal{D} \mathcal{R}] - \bar{\delta}_\mathcal{R} \text{Tr}[\bar{\mathcal{R}} \mathcal{R}] + \frac{\tilde{b}_D}{2B_0} \text{Tr}[\bar{\mathcal{R}} \{\chi_+, \mathcal{R}\}] \\ & + \frac{\tilde{b}_F}{2B_0} \text{Tr}[\bar{\mathcal{R}} [\chi_+, \mathcal{R}]] + \frac{\tilde{b}_0}{2B_0} \text{Tr}[\bar{\mathcal{R}} \mathcal{R}] \text{Tr}[\chi_+] \\ & - 2r_D (\text{Tr}[\bar{\mathcal{R}} (v_\mu S_\nu - v_\nu S_\mu) \{f_+^{\mu\nu}, B\}]) \\ & + \text{Tr}[\bar{\mathcal{R}} (v_\mu S_\nu - v_\nu S_\mu) \{f_+^{\mu\nu}, R\}] \\ & - 2r_F (\text{Tr}[\bar{\mathcal{R}} (v_\mu S_\nu - v_\nu S_\mu) [f_+^{\mu\nu}, B]]) \\ & + \text{Tr}[\bar{\mathcal{R}} (v_\mu S_\nu - v_\nu S_\mu) [f_+^{\mu\nu}, \mathcal{R}]]. \end{aligned} \quad (9)$$

The second to fifth terms of $\mathcal{L}_\mathcal{R}$ give the average residual mass and mass splitting among the $(1/2)^-$ baryon octet. Constants r_D and r_F are electromagnetic coupling strengths between B and \mathcal{R} , and $f_+^{\mu\nu}$ is the chiral field strength tensor of the electromagnetic field that, in the SU(3) version of ChPT, is given by [29]

$$f_+^{\mu\nu} = -e [\xi^\dagger Q \xi + \xi Q \xi^\dagger] F^{\mu\nu} \quad (10)$$

with $e > 0$. The reason we include r_D and r_F terms even though they are formally $1/m_N$ suppressed is that they will then be compensated by small denominator δ_B factors in pole diagrams.

Next I introduce the relevant weak Lagrangian that gives rise to the nucleon EDM. As the only CP-violating effect in the SM is the complex phase in the CKM matrix, the strange quark must be included. The CP phase is attached to various $|\Delta S| = 1$ four-quark operators that are responsible for kaon decay and nonleptonic hyperon decays. It is well known that the product of two charged weak currents could transform as $(8_L, 1_R)$ or $(27_L, 1_R)$ under the SU(3) chiral rotation.

²In the sense that it only depends on the residual momentum.

Extra $|\Delta S| = 1$ operators could be induced via gluonic or electroweak penguin diagrams. The former transforms as $(8_L, 1_R)$ while the latter may introduce a $(8_L, 8_R)$ component that is, however, suppressed by the smallness of the fine structure constant. Furthermore, since $(8_L, 1_R)$ operators have isospin $I = 1/2$ while $(27_L, 1_R)$ operators can have both $I = 1/2$ and $I = 3/2$ components, we would naturally expect the latter to be subdominant as compared to the $(8_L, 1_R)$ operators. Otherwise the $I = 3/2$ channel would be as important as the $I = 1/2$ channel in nonleptonic decay processes, violating the experimentally observed $|\Delta I| = 1/2$ dominance in these processes. Hence, effective operators I introduce later should also transform as $(8_L, 1_R)$.

The pure mesonic Lagrangian that triggers the $|\Delta I| = 1/2$ kaon decay channel is given by [31]

$$\mathcal{L}_8 = g_8 e^{i\varphi} \text{Tr}[\lambda_+ D_\mu U D^\mu U^\dagger] + \text{H.c.}, \quad (11)$$

where $\lambda_+ = (\lambda_6 + i\lambda_7)/2$. The non zero value of φ introduces the CP-violating effect. Meanwhile, the corresponding baryonic operator that triggers the nonleptonic hyperon decay is given by [36]

$$\begin{aligned} \mathcal{L}_w^{(s)} = & h_D e^{i\varphi_D} \text{Tr}[\bar{B}\{\xi^\dagger \lambda_+ \xi, B\}] \\ & + h_F e^{i\varphi_F} \text{Tr}[\bar{B}\{\xi^\dagger \lambda_+ \xi, B\}] + \text{H.c.} \end{aligned} \quad (12)$$

Here the superscript (s) indicates that these operators mediate S -wave decays. In principle there is a counterpart operator with the Dirac structure γ_5 , which is time-reversal odd and is proportional to the complex phase in the CKM matrix. I do not need this extra operator because it vanishes at leading order in the HB expansion upon the nonrelativistic reduction of the Dirac structure. Also, our definitions of h_D and h_F here are slightly different from [36] as we take h_D, h_F to be real, with the complex phases explicitly factored out.

Finally, for the purpose of including pole-diagram contributions, I need the weak Lagrangian that triggers the $B - \mathcal{R}$ transition. The lowest-order Lagrangian is given by [37]

$$\begin{aligned} \mathcal{L}_w^{B\mathcal{R}} = & i w_D e^{i\tilde{\varphi}_D} \text{Tr}[\bar{\mathcal{R}}\{h_+, B\}] \\ & + i w_F e^{i\tilde{\varphi}_F} \text{Tr}[\bar{\mathcal{R}}\{h_+, B\}] + \text{H.c.}, \end{aligned} \quad (13)$$

where $h_+ \equiv \xi^\dagger \lambda_+ \xi + \xi^\dagger \lambda_- \xi$. The counterpart with a γ_5 structure similarly vanishes at leading order in the HB expansion.

III. DETERMINATION OF THE LECS

There are altogether 12 LECs that enter into the estimate for the nucleon EDM: seven interaction strengths $\{r_D, r_F, g_8, h_D, h_F, w_D, w_F\}$ and five CP-violating phases $\{\varphi, \varphi_D, \varphi_F, \tilde{\varphi}_D, \tilde{\varphi}_F\}$. They are either extracted from experiments or obtained by theoretical modeling.³

Pure electromagnetic $B - \mathcal{R}$ transition coupling strengths r_D and r_F are fitted to electromagnetic decays of $(1/2)^-$ resonances. The authors of Ref. [35] obtain

$$er_D = 0.033 \text{ GeV}^{-1}, \quad er_F = -0.046 \text{ GeV}^{-1}. \quad (14)$$

³Unfortunately, none of these LECs in the literature come with error bars, so I cannot estimate the error introduced by the fitting of LECs.

The constant g_8 is fitted to the $K_s^0 \rightarrow \pi^+ \pi^-$ decay rate, ignoring the small CP-violating effect [38], giving

$$g_8 = 6.84 \times 10^{-10} \text{ GeV}^2. \quad (15)$$

The CP phase φ is, up to a negative sign, the phase of the $K^0 \rightarrow \pi\pi (I = 0)$ decay amplitude:

$$\varphi = -\xi_0 = -\frac{\text{Im } A_0}{\text{Re } A_0} \quad (16)$$

In principle one could extract ξ_0 from the measurement of the CP-violating parameter ϵ' in the kaon decay. However, ϵ' is a linear combination of ξ_0 and another CP-violating phase, ξ_2 , of the $I = 3/2$ channel. Simple estimation [31] suggests that ξ_2 is of the same order as ξ_0 , making ξ_0 hard to extract directly from the experiment. I therefore refer to theoretical estimation based on the large- N_c approach [39] which gives

$$\varphi = -\xi_0 \approx -\sqrt{2}|\epsilon| \times (-6 \times 10^{-2}) \approx 1.89 \times 10^{-4} \approx 6.4J, \quad (17)$$

where $J = (2.96_{-0.16}^{+0.20}) \times 10^{-5}$ [38] is the Jarlskog invariant [40]. It is worthwhile to mention that, in Ref. [18] the uncertainty of J spans an order of magnitude leading to the main source of the error in the estimate of the neutron EDM during that time. Today, J is determined with much higher precision so the associated uncertainty is subleading compared to uncertainties due to higher-order effects in the HB expansion and unknown short-distance counterterms, which we will discuss later.

The four remaining interaction strengths h_D, h_F, w_D, w_F were determined in [37] by simultaneously fitting them to the s - and p -wave amplitudes of nonleptonic hyperon decays:

$$\begin{aligned} h_D &\approx 0.44 \times 10^{-7} \text{ GeV}, & h_F &\approx -0.50 \times 10^{-7} \text{ GeV}, \\ w_D &\approx -1.8 \times 10^{-7} \text{ GeV}, & w_F &\approx 2.3 \times 10^{-7} \text{ GeV}. \end{aligned} \quad (18)$$

The last two constants were determined by setting $m_{\mathcal{R}} \approx 1535 \text{ MeV}$.

Finally, I need to know the four remaining CP phases $\{\varphi_D, \varphi_F, \tilde{\varphi}_D, \tilde{\varphi}_F\}$. These phases have been considered in Ref. [15], but their treatments are less satisfactory due to the neglect of the operator mixing effect and a certain outdated approximation of the small top-quark mass assumption. In order to improve upon that, I review a more recent work done in Ref. [36] that determined $\{\varphi_D, \varphi_F\}$ and apply scaling arguments to provide an estimate of $\{\tilde{\varphi}_D, \tilde{\varphi}_F\}$. Reference [36] pointed out that, after considering operator mixing and renormalization group running, the dominant operator that gives rise to the CP-violating phase in the $|\Delta S| = 1$, $|\Delta I| = 1/2$ sector is given by

$$\hat{Q}_6 = -2 \sum_q \bar{d}(1 + \gamma_5) q \bar{q}(1 - \gamma_5) s. \quad (19)$$

Reference [36] then computed the factorizable and nonfactorizable contributions to φ_D, φ_F induced by \hat{Q}_6 . Here ‘‘factorizable’’ means to regard \hat{Q}_6 as a product of two chiral quark densities and match it to chiral operators. The matching is done by realizing that $\bar{q}_R q_L \sim \partial \mathcal{L}_{QCD} / \partial m_q = \partial \mathcal{L}_{\text{chiral}} / \partial m_q$. On the other hand, the ‘‘nonfactorizable’’ contribution is obtained

simply by taking the hadronic matrix element of \hat{Q}_6 using the quark model. These two contributions are distinct because the factorizable piece contains a factor of chiral quark condensate $F_\pi^2 B_0$ through

$$\begin{aligned} \langle 0 | \bar{q}_L^i q_R^j \bar{q}_R^k q_L^l | B \bar{B}' \rangle &\sim \langle 0 | \bar{q}_L^i q_R^j | 0 \rangle \langle 0 | \bar{q}_R^k q_L^l | B \bar{B}' \rangle \\ &= -\frac{1}{2} F_\pi^2 B_0 \delta_{ij} \langle 0 | \bar{q}_R^k q_L^l | B \bar{B}' \rangle \end{aligned} \quad (20)$$

while the same quantity never appears in a quark model calculation. Combining the two, the authors found $\text{Im}(h_D \exp i\varphi_D) \approx -2.2$, $\text{Im}(h_F \exp i\varphi_F) \approx 6.1$, both in units of $\sqrt{2} F_\pi G_F m_\pi^2 J$. This leads to

$$\varphi_D \approx -1.5J, \quad \varphi_F \approx -3.6J. \quad (21)$$

It is straightforward to see that $\tilde{\varphi}_D$ and $\tilde{\varphi}_F$ receive no factorizable contribution. This is because it would require terms like $\bar{R} m_q B$ to appear in the strong chiral Lagrangian. Such terms would violate parity and therefore cannot exist. For the nonfactorizable part, my strategy is the following: first I compute the matrix elements $\langle \mathcal{R} | \hat{Q}_6 | B \rangle$ and $\langle B' | \hat{Q}_6 | B \rangle$ using the quark model to find their ratio. Then, I use this ratio to infer the value of the nonfactorizable part of $\tilde{\varphi}_D$, $\tilde{\varphi}_F$ by appropriately scaling the nonfactorizable part of φ_D , φ_F given in Ref. [36].

To obtain an estimate of hadronic matrix elements I adopt the harmonic oscillator model [34]. The structure of the spin-flavor wavefunction of the baryon octet leads to the following ratio:

$$\langle n^* | \hat{Q}_6 | \Sigma^0 \rangle : \langle n^* | \hat{Q}_6 | \Lambda \rangle : \langle p^* | \hat{Q}_6 | \Sigma^+ \rangle = 1 : \sqrt{3} : -\sqrt{2}, \quad (22)$$

which requires that $w_F \tilde{\varphi}_F = (1/3) w_D \tilde{\varphi}_D$ in our chiral Lagrangian. I also obtain the ratio between $B - B'$ and $B - \mathcal{R}$ matrix elements:

$$\frac{\langle p^* | \hat{Q}_6 | \Sigma^+ \rangle}{\langle p | \hat{Q}_6 | \Sigma^+ \rangle} = -\sqrt{\frac{2}{3}} \frac{1}{m R_0}. \quad (23)$$

where $m \approx 0.34$ GeV, $R_0 \approx 2.7$ GeV⁻¹ are harmonic oscillator parameters. With this ratio and the nonfactorizable contribution to φ_D, φ_F given in [36], I obtain the nonfactorizable contribution to $\tilde{\varphi}_D, \tilde{\varphi}_F$:

$$\tilde{\varphi}_D \approx 0.04J, \quad \tilde{\varphi}_F \approx -0.01J. \quad (24)$$

These phases are about two orders of magnitude smaller than the three other CP phases because they are not enhanced by the chiral quark condensate. Therefore, I disregard them in the rest of our calculation.

To end this section, I point out that there is an important sign issue in the determination of LECs. Since LECs are fitted to experiments that only involve squared amplitudes, an overall undetermined sign is left ambiguous. Therefore, if two sets of LECs are fitted separately to two unrelated experiments (for example, $\{r_D, r_F\}$ are to fit to baryon electromagnetic transitions and $\{h_D, h_F, w_D, w_F\}$ are to fit to non leptonic hyperon decays), there is no unique way to determine the relative sign between these two sets of LECs. This introduces an extra uncertainty because a change of a relative sign can

turn a constructive interference to destructive and vice versa. I will discuss the impact of this uncertainty in the last section.

IV. ONE-LOOP CONTRIBUTION

In this section I present analytic and numerical results of the one-loop contribution to the proton and neutron EDM using HBchPT. The nucleon EDM d_N is defined by the term linear in the incoming photon momentum q of the P- and T-violating $NN\gamma$ amplitude

$$iM \equiv -2d_N v \cdot \varepsilon \bar{u}_N S \cdot q u_N. \quad (25)$$

Here ε^μ is the photon polarization vector. Note that the equation has been simplified by applying the on-shell condition to the nucleon: $v \cdot q = -q^2/2m_N \rightarrow 0$.

Since each weak interaction vertex has $|\Delta S| = 1$, I need at least two insertions of weak interaction vertices to obtain an EDM that is flavor diagonal. Most one-loop integrals are UV divergent and are regularized using the $\overline{\text{MS}}$ scheme in which the combination

$$L \equiv \frac{2}{4-d} - \gamma + \ln(4\pi) \quad (26)$$

is subtracted. Also, since all CP-violating phases $\{\varphi_i\}$ are small, I use the small-angle approximation $\sin \varphi_i \approx \varphi_i$. Finally, following the usual spirit of ChPT, during the calculation of loops we assume that the heavy DOFs could be integrated out and that their effects showing up in the LECs of the effective operators consist of lighter DOFs.⁴ Hence what enter the loops are the lightest DOFs, which in our case are the pseudoscalar meson octet and the ground-state $(1/2)^+$ baryon octet.

There are four distinct types of one-loop diagrams (see Fig. 1) that give nonzero contribution to the nucleon EDM. (Diagrams of other kinds are all vanishing at leading order in the HB expansion. See the Appendix for the argument.) Figures 1(a)–1(c) (plus reflections) show contributions to both neutron and proton EDMs. For the neutron, it reads

$$\begin{aligned} d_n^{1\text{-loop}} &= -\frac{eg_s(Dh_D\{\varphi - \varphi_D\} + Fh_F\{\varphi - \varphi_F\})}{4\pi^2 F_\pi^4 (m_\pi^2 - m_K^2)} \\ &\times \left(m_\pi^2 \ln \frac{m_\pi^2}{\mu^2} - \{\pi \leftrightarrow K\} \right) \\ &- \frac{\delta_\Sigma eg_s(D - F)(h_D\{\varphi - \varphi_D\} + h_F\{\varphi_F - \varphi\})}{4\pi^2 F_\pi^2 (m_\pi^2 - m_K^2)} \\ &\times \left(m_\pi^2 \frac{\arctan \frac{\sqrt{m_\pi^2 - \delta_\Sigma^2}}{\delta_\Sigma}}{\sqrt{m_\pi^2 - \delta_\Sigma^2}} - \{\pi \leftrightarrow K\} \right). \end{aligned} \quad (27)$$

I found that all terms analytic in quark masses cancel each other. Also notice that there is no extra singularity in the limit $m_K \rightarrow m_\pi$ or $\delta_B \rightarrow 0$. Numerical estimation with $\mu = m_N$

⁴The reader should anyway be alerted that this may not always be the case. For example, in Ref. [43] the authors pointed out that one needs to include the baryon decuplet in order to reconcile with the result of the large N_c expansion.

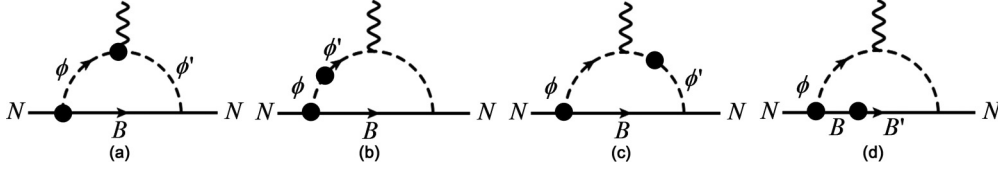


FIG. 1. One-loop contributions to the nucleon EDM. Each round dot denotes a $|\Delta S| = 1$ weak insertion. Figs. 1(a)–1(c) (and reflections) contribute to both neutron and proton EDMs, while Fig. 1(d) (and reflection) contributes only to proton EDM.

gives

$$|d_n^{1\text{-loop}}| = 1.5 \times 10^{-32} e \text{ cm}. \quad (28)$$

Similar calculations are done for the proton EDM. Figures 1(a)–1(c) give

$$d_p^{1\text{-loop},1} = \frac{eg_8(D\{h_D[\varphi - \varphi_D] + 3h_F[\varphi - \varphi_F]\} + 3F\{h_D[\varphi - \varphi_D] + h_F[\varphi_F - \varphi]\})}{24\pi^2 F_\pi^4 (m_\pi^2 - m_K^2)} \left(m_\pi^2 \ln \frac{m_\pi^2}{\mu^2} - \{\pi \leftrightarrow K\} \right) - \frac{\delta_\Sigma eg_8(D - F)(h_D\{\varphi - \varphi_D\} + h_F\{\varphi_F - \varphi\})}{8\pi^2 F_\pi^4 (m_\pi^2 - m_K^2)} \left(m_\pi^2 \frac{\arctan \frac{\sqrt{m_\pi^2 - \delta_\Sigma^2}}{\delta_\Sigma}}{\sqrt{m_\pi^2 - \delta_\Sigma^2}} - \{\pi \leftrightarrow K\} \right) - \frac{\delta_\Lambda eg_8(D + 3F)(h_D\{\varphi - \varphi_D\} + 3h_F\{\varphi - \varphi_F\})}{24\pi^2 F_\pi^4 (m_\pi^2 - m_K^2)} \left(m_\pi^2 \frac{\arctan \frac{\sqrt{m_\pi^2 - \delta_\Lambda^2}}{\delta_\Lambda}}{\sqrt{m_\pi^2 - \delta_\Lambda^2}} - \{\pi \leftrightarrow K\} \right). \quad (29)$$

There is one extra type of diagram contributing to the proton EDM, corresponding to two insertions of h_i vertices [Fig. 1(d)]. The corresponding diagrams do not generate the neutron EDM simply because there is no appropriate nonvanishing combination of B, B', ϕ . This diagram for the proton EDM gives

$$d_p^{1\text{-loop},2} = - \frac{eh_D h_F (D - F)(\varphi_D - \varphi_F)(\pi - 2 \arctan \frac{\delta_\Sigma}{\sqrt{m_K^2 - \delta_\Sigma^2}})}{16\pi^2 F_\pi^2 \sqrt{m_K^2 - \delta_\Sigma^2}} - \frac{eh_D h_F (D + 3F)(\varphi_D - \varphi_F)(\pi - 2 \arctan \frac{\delta_\Lambda}{\sqrt{m_K^2 - \delta_\Lambda^2}})}{48\pi^2 F_\pi^2 \sqrt{m_K^2 - \delta_\Lambda^2}}. \quad (30)$$

This contribution is interesting since it is UV finite. It depends nonanalytically on quark masses and hence uniquely characterizes long-distance physics.⁵ Numerically, these give

$$|d_p^{1\text{-loop},1}| = 6.1 \times 10^{-33} e \text{ cm}, \\ |d_p^{1\text{-loop},2}| = 1.1 \times 10^{-32} e \text{ cm}. \quad (31)$$

I choose to present numerical results of $d^{1\text{-loop},1}$ and $d^{1\text{-loop},2}$ separately because the former is proportional to $g_8 h_i$ while the latter is proportional to $h_i h_j$. Since the relative sign between g_8 and h_i is experimentally undetermined, these two terms can either add to or subtract from each other.

As a short conclusion, I stress once again that within the HBchPT formalism, my analytic results of one-loop diagrams, Eqs. (27), (29), and (30), fully respect power counting as no powers of m_B appear in the numerator upon carrying out loop integrals. This is in contrast with the relativistic calculation done in Ref. [18], in which the authors include diagrams involving MDM-like coupling that should have an explicit $1/m_B$ suppression according to the power counting, but is

canceled by a factor of m_B appearing in the numerator coming from the loop integral.

Finally let me discuss the effect of counterterms. Since $d_n^{1\text{-loop}}$ and $d_p^{1\text{-loop},1}$ are UV divergent, I need to introduce corresponding counterterms d_n^0, d_p^0 to absorb the infinities. These counterterms are generated by short-distance physics. Therefore their precise values cannot be calculated. To estimate the size of these counterterms we perform a naive dimensional analysis (NDA). Following [41], there are ten $\Delta S = 1$ four-quark operators that mix under renormalization. The effective Hamiltonian can be written as

$$H_{\text{eff}}^{\Delta S=1} = \frac{G_F}{\sqrt{2}} V_{ud} V_{us}^* \sum_{i=1}^{10} C_i(\mu) \hat{Q}_i(\mu) + \text{H.c.} \quad (32)$$

Under conditions that $\Lambda_{\text{QCD}} \approx 0.2 \text{ GeV}$, $\mu = 1 \text{ GeV}$, and the top-quark mass $m_t = 174 \text{ GeV}$, the largest flavor-diagonal CP-violating effect comes from the product of \hat{Q}_2 and \hat{Q}_6 with Wilson coefficients $C_2 = 1.31 - 0.044\tau$ and $C_6 = -0.011 - 0.080\tau$, where $\tau = -V_{td} V_{ts}^* / V_{ud} V_{us}^*$. This gives

$$d_p^0, d_n^0 \sim \frac{1}{16\pi^2} \frac{G_F^2}{2} |V_{ud} V_{us}^*|^2 \text{Im}(C_2 C_6^*) \Lambda_\chi^3 \approx 4 \times 10^{-32} e \text{ cm}. \quad (33)$$

⁵One can show that Eq. (30) remains real even when $\delta_K, \delta_\Lambda > m_K$ by using the identity $\arctan z = \frac{1}{2i} \ln \frac{1+iz}{1-iz}$.

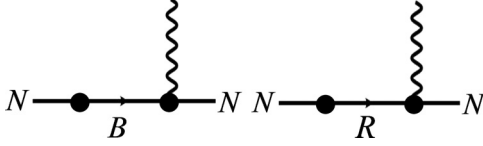


FIG. 2. Class I pole diagrams (with reflections).

Here $1/16\pi^2$ is a necessary loop factor while the factor Λ_χ^3 is included to achieve the correct mass dimension. I choose $\Lambda_\chi \sim 1$ GeV instead of some other scale like $\Lambda_{\text{QCD}} \sim 200$ MeV to provide a conservative upper limit for d_n^0 and d_p^0 . This analysis shows that the short-distance contribution to the nucleon EDM could be as large as the long-distance contribution.⁶ However the NDA estimation is rarely trustable and it may happen that some accidental cancelations could suppress the actual value of d_n^0, d_p^0 from what is expected in Eq. (33). In this sense, a detailed study of the long-distance contribution is worthwhile because it sets a solid bound below which any measurable nucleon EDM could be safely regarded as being consistent with the SM prediction.

V. POLE CONTRIBUTION

Next I estimate the contribution of pole diagrams to the nucleon EDM. For baryon intermediate states, I include the flavor octet part of the $(56, 0^+)$ and $(70, 1^-)$ baryon supermultiplets. Here I adopt the standard spin-flavor SU(6) notation (\mathcal{D}, L^P) where \mathcal{D} is the dimension of the SU(6)

$$\begin{aligned}
 d_n^{\text{pole}} &= \frac{4er_D}{9\delta_\Lambda\delta_{\Lambda^*}\delta_{N^*}\delta_{\Sigma^*}\delta_\Sigma} (h_D\varphi_D\{3w_F[2\delta_{\Lambda^*}\delta_{\Sigma^*}(\delta_\Lambda - \delta_\Sigma) + \delta_{N^*}\{\delta_{\Lambda^*}(\delta_\Lambda + \delta_\Sigma) \\
 &\quad + \delta_{\Sigma^*}(\delta_\Sigma - 3\delta_\Lambda)\}] - w_D[2\delta_{\Lambda^*}\delta_{\Sigma^*}(3\delta_\Lambda + \delta_\Sigma) + \delta_{N^*}\{3\delta_{\Lambda^*}(\delta_\Lambda + \delta_\Sigma) + \delta_{\Sigma^*}(3\delta_\Lambda - \delta_\Sigma)\}]) \\
 &\quad + 3h_F\varphi_F\{w_D[2\delta_{\Lambda^*}\delta_{\Sigma^*}(\delta_\Lambda - \delta_\Sigma) + \delta_{N^*}\{\delta_{\Lambda^*}(\delta_\Lambda - 3\delta_\Sigma) + \delta_{\Sigma^*}(\delta_\Lambda + \delta_\Sigma)\}] \\
 &\quad + w_F[\delta_{N^*}\{3\delta_{\Sigma^*}(\delta_\Lambda + \delta_\Sigma) - \delta_{\Lambda^*}(\delta_\Lambda - 3\delta_\Sigma)\} - 2\delta_{\Lambda^*}\delta_{\Sigma^*}(\delta_\Lambda + 3\delta_\Sigma)\}), \\
 d_p^{\text{pole}} &= -\frac{8e(\delta_{N^*} - \delta_{\Sigma^*})(r_D + 3r_F)(w_D - w_F)(h_D\varphi_D - h_F\varphi_F)}{3\delta_{N^*}\delta_{\Sigma^*}\delta_\Sigma}. \tag{34}
 \end{aligned}$$

In the expression above I have neglected the two small phases $\tilde{\varphi}_D$ and $\tilde{\varphi}_F$. Note that Eq. (34) diverges in the $\delta \rightarrow 0$ limit. This simply indicates that nondegenerate perturbation theory fails in this limit and one needs to switch to degenerate perturbation theory. Numerically, Eq. (34) gives

$$|d_n^{\text{pole}}| \approx |d_p^{\text{pole}}| \approx 1.4 \times 10^{-32} \text{ e cm}. \tag{35}$$

Numerical results are summarized in Table I. I caution the readers that all these numbers are only indicative of the size, because I have not yet addressed the sign ambiguities plaguing the determination of certain LECs as emphasized at the end of Sec. III. This will be done in the next section.

⁶A followup work from the author to compute these short-distance contributions within certain nucleon model framework is currently in progress.

representation, L is the orbital angular momentum, and p is the parity. For generality, we first write down all possible pole configurations that can contribute and divide it into two classes: Class I are those in which the photon vertex involves a weak insertion and Class II are those in which the photon vertex is purely electromagnetic (see Figs. 2 and 3).

I want to single out the leading pole diagrams. First, one would expect that Class I contributions are much smaller than Class II for two reasons: (1) the weak photon vertex in Class I diagrams is due to the transition quark magnetic dipole moment (MDM) that contains a $m_s + m_d$ suppression factor or the transition quark EDM that is suppressed by $m_s - m_d$ (the latter, which vanishes if $m_s \rightarrow m_d$, is an explicit demonstration of Hara's theorem [33]); (2) Class II diagrams have one more pole in the denominator. With these observations I may safely discard Class I diagrams since they are subleading.

Within Class II, Figs. 3(a)–3(d) can be shown to have an extra $1/m_N$ suppression [42]. These four diagrams involve MDM-like baryon radiative transition vertices that have the structure of $(1/m_B)\epsilon^{\mu\nu\alpha\beta}v_\nu q_\alpha S_\beta$ at leading order. This structure is orthogonal to the EDM structure $v^\mu S \cdot q$ so it cannot generate an EDM. Therefore in order to obtain an EDM one needs to go to the next order in the HB expansion leading to an extra $1/m_N$ suppression, so I can discard these four diagrams. Finally, Fig. 3(e) is smaller than Figs. 3(f) and 3(g) due to an extra propagator of a heavy excited state R . After all these considerations, I only need to evaluate Figs. 3(f) and 3(g). Using Feynman rules obtained from the Lagrangian in Sec. II, I obtain

VI. DISCUSSION AND SUMMARY

Now I consider the uncertainty due to the undetermined relative sign between different groups of LECs. Since r_D and r_F are fitted simultaneously to the electromagnetic decay of $(1/2)^-$ resonance they should be multiplied by a common undetermined sign factor $\delta_r = \pm 1$. The constant g_8 is fitted to the kaon decay rate, so it should carry a separate sign factor δ_g . Its phase φ , however, is determined theoretically so it does not have a sign ambiguity. The four remaining interaction strengths $\{h_D, h_F, w_D, w_F\}$ are fitted simultaneously to s - and p -wave amplitudes of the hyperon nonleptonic decay, so they should carry a common undetermined sign factor δ_{hw} . Their corresponding phases are determined by first calculating $\text{Im}\{h_i \exp i\varphi_i\}$ and $\text{Im}\{w_i \exp i\tilde{\varphi}_i\}$ theoretically and then by dividing them by the experimentally determined $\{h_i, w_i\}$ so the four remaining phases $\{\varphi_D, \varphi_F, \tilde{\varphi}_D, \tilde{\varphi}_F\}$ should

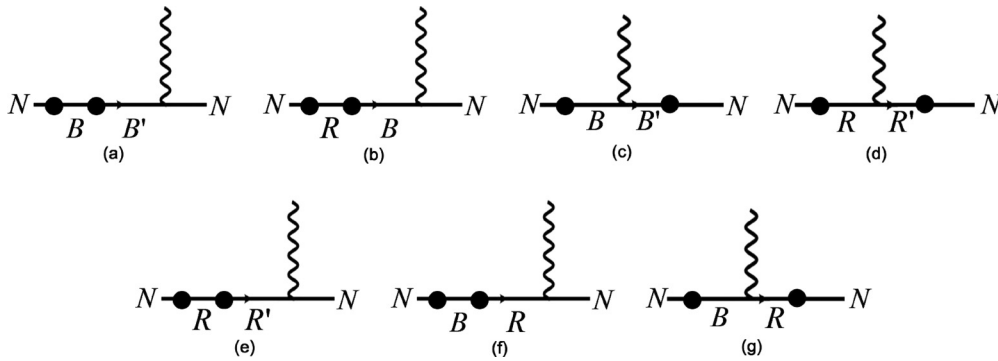


FIG. 3. Class II pole diagrams (with reflections).

also carry the same sign factor δ_{hw} . Summing up loop and pole diagram contributions and allowing $\{\delta_r, \delta_g, \delta_{hw}\}$ to freely change between 1 and -1 , I obtain a range of possible d_n and d_p :

$$\begin{aligned} 8.7 \times 10^{-34} < |d_n| < 2.8 \times 10^{-32} \text{ e cm}, \\ 3.3 \times 10^{-33} < |d_p| < 3.3 \times 10^{-32} \text{ e cm}. \end{aligned} \quad (36)$$

The surprisingly small lower bounds of $|d_n|, |d_p|$ are due to an accidental cancellation between loop and pole-diagram contributions for a very specific set of $\{\delta_i\}$. There is no reason to believe that this cancellation persists at higher order. To estimate the size of higher-order contributions, I recall that the HB-expansion parameter is of order $m_K/m_N \sim 0.5$. Therefore to be conservative, I could assign a 100% error due to the next-to-leading-order (NLO) effects in the HB expansion. Also, by looking at Table I one can see that both loop and pole diagrams are of order 10^{-32} e cm. So if I assume no fine cancellation between these two parts after adding the NLO contributions from the HB expansion, then I should expect the long-distance contribution to the nucleon EDM to lie within the range

$$1 \times 10^{-32} < \{|d_n|, |d_p|\} < 6 \times 10^{-32} \text{ e cm}. \quad (37)$$

My estimated upper bound for d_n is about half the corresponding value predicted in [18]. Equation (37) is three (four) orders of magnitude smaller than the proposed precision level of the future proton (neutron) EDM experiments.

To summarize, even though it is well known that the nucleon EDM induced by the standard model CKM matrix is well below the limit of our current experimental precision, it is still worth a thorough study as it is currently the only source of intrinsic EDMs in nature whose existence is certain. I re-analyze previous works on chiral loop and pole diagram contributions to the nucleon EDM using HBchPT

TABLE I. Different contributions to the SM neutron and proton EDMs in units of e cm, assuming the signs of LECs are those given in Sec. III.

Nucleon	EDM		
	$ d_N^{1\text{-loop},1} $	$ d_N^{1\text{-loop},2} $	$ d_N^{\text{pole}} $
neutron	1.5×10^{-32}	0	1.4×10^{-32}
proton	6.1×10^{-33}	1.1×10^{-32}	1.4×10^{-32}

at the leading order in HB expansion, with an up-to-date determination of relevant LECs that enter our calculation. Combined with the uncertainty due to unknown relative signs of LECs and an estimate of higher-order contributions, I obtain the range for the long-distance contribution to the nucleon EDM in Eq. (37). Although an incalculable short-distance physics which appears as counterterms in our work could be as large as the long-distance contribution, the study of the long-distance contribution is still worthwhile as it provides a safe borderline below which any nucleon EDM is consistent with the SM prediction. Finally, there are several ways to improve upon the estimate carried out in this work. For instance, a combined analysis of lattice simulations and better experimental measurements of various hadronic decay processes is expected to provide a better control of both the magnitudes and signs of the required LECs. If the LECs could be determined more precisely, then a complete analysis of NLO effects in the HB expansion would be much desired to further restrict the allowed range of d_n and d_p .

ACKNOWLEDGMENTS

The author would like to thank Michael J. Ramsey-Musolf, John F. Donoghue, and Barry R. Holstein for many useful discussions. The author is also grateful to Hiren H. Patel and Graham White for carefully reading the manuscript and providing extensive valuable feedback. This work is supported in part by the U.S. Department of Energy under Contract No. DE-SC0011095.

APPENDIX: VANISHING ONE-LOOP DIAGRAMS

Here I will show that all one-loop diagrams, other than those in Fig. 1, do not give rise to the nucleon EDM, at least at leading order in the HB-expansion.

All other possible one-loop diagrams beside those I have calculated are summarized in Fig. 4. Since the weak Lagrangian used in my work does not involve covariant derivatives of baryon fields, any baryon-photon coupling term has to arise from the ordinary P- and T-conserving Lagrangian.

For Fig. 4(a), the photon vertex must arise from Dirac coupling since an MDM coupling is suppressed by $(1/m_N)^2$ as pointed out in [42]. Since the Dirac coupling is independent of the photon momentum q , one can define loop momenta in a way such that the dependence of q only appears in the baryon

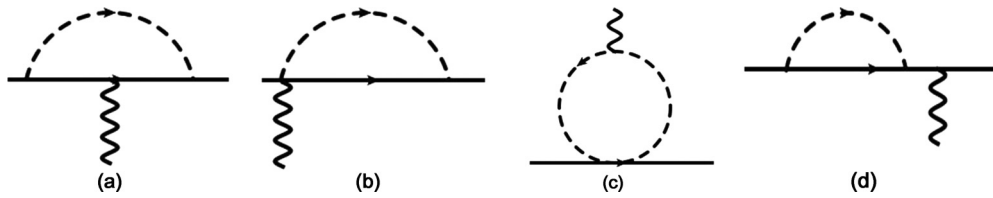


FIG. 4. One-loop diagrams that vanish at LO HB χ PT. The weak vertices could be placed at any allowed position and therefore are not explicitly shown.

propagator. However, using the on-shell condition $v \cdot q = 0$, the baryon propagator is actually q independent and therefore so is the whole diagram. As a result, Fig. 4(a) cannot generate an EDM that is linear in q .

For Fig. 4(b), at leading order in the HB expansion the $BB'\phi\gamma$ vertex is proportional to S^μ , so it cannot generate an EDM because the latter is proportional to v^μ which is perpendicular to S^μ .

For Fig. 4(c), first I note that the $BB'\phi\phi'$ vertex cannot come from the D or F term of the ordinary chiral Lagrangian because that would violate parity. Therefore it can only come

from $\mathcal{L}_w^{(s)}$. In this case, it can only be parity conserving and time-reversal conserving (PCTC), or parity conserving and time-reversal violating (PCTV). So in order to get an EDM which is PVTV, one needs to place another PVTC or PVTV vertex in some other part of the diagram. This cannot be done because all $\phi\phi'$ and $\phi\phi'\gamma$ operators I have are parity conserving.

For Fig. 4(d), one could generate an EDM by coupling the resulting complex mass term of the baryon to its MDM. But again this contribution is suppressed by $(1/m_N)^2$ and should be discarded at leading order in the HB expansion.

-
- [1] A. D. Sakharov, *Pisma Zh. Eksp. Teor. Fiz.* **5**, 32 (1967) [*JETP Lett.* **5**, 24 (1967)]; *Usp. Fiz. Nauk* **161**, 61 (1991) [*Sov. Phys. Usp.* **34**, 392 (1991)].
- [2] J. H. Smith, E. M. Purcell, and N. F. Ramsey, *Phys. Rev.* **108**, 120 (1957).
- [3] J. Baron *et al.* (ACME Collaboration), *Science* **343**, 269 (2014).
- [4] W. C. Griffith, M. D. Swallows, T. H. Loftus, M. V. Romalis, B. R. Heckel, and E. N. Fortson, *Phys. Rev. Lett.* **102**, 101601 (2009).
- [5] C. A. Baker, D. D. Doyle, P. Geltenbort, K. Green, M. G. D. van der Grinten, P. G. Harris, P. Iaydjiev, S. N. Ivanov *et al.*, *Phys. Rev. Lett.* **97**, 131801 (2006).
- [6] I. Altarev, G. Ban, G. Bison, K. Bodek, M. Burghoff, M. Cvijovic, M. Daum, P. Fierlinger *et al.*, *Nucl. Instrum. Methods A* **611**, 133 (2009).
- [7] A. P. Serebrov *et al.*, *Nucl. Instrum. Methods A* **611**, 263 (2009).
- [8] K. Kumar, Z.-T. Lu, and M. J. Ramsey-Musolf, [arXiv:1312.5416](https://arxiv.org/abs/1312.5416).
- [9] A. Lehrach, B. Lorentz, W. Morse, N. Nikolaev, and F. Rathmann, [arXiv:1201.5773](https://arxiv.org/abs/1201.5773).
- [10] Y. K. Semertzidis (Storage Ring EDM Collaboration), [arXiv:1110.3378](https://arxiv.org/abs/1110.3378).
- [11] M. Pospelov, talk given at the Winter Workshop on Electric Dipole Moment (EDMs13), February 13–15, 2013, Fermilab (unpublished).
- [12] E. P. Shabalin, *Yad. Fiz.* **32**, 443 (1980) [*Sov. J. Nucl. Phys.* **32**, 228 (1980)].
- [13] A. Czarnecki and B. Krause, *Phys. Rev. Lett.* **78**, 4339 (1997).
- [14] G. Barton and E. D. White, *Phys. Rev.* **184**, 1660 (1969).
- [15] M. B. Gavela, A. Le Yaouanc, L. Oliver, O. Pene, J. C. Raynal, and T. N. Pham, *Phys. Lett. B* **109**, 215 (1982).
- [16] M. B. Gavela, A. Le Yaouanc, L. Oliver, O. Pene, J. C. Raynal, and T. N. Pham, *Phys. Lett. B* **109**, 83 (1982).
- [17] I. B. Khriplovich and A. R. Zhitnitsky, *Phys. Lett. B* **109**, 490 (1982).
- [18] X.-G. He, B. H. J. McKellar, and S. Pakvasa, *Int. J. Mod. Phys. A* **4**, 5011 (1989); **6**, 1063 (1991).
- [19] T. Mannel and N. Uraltsev, *Phys. Rev. D* **85**, 096002 (2012).
- [20] E. E. Jenkins and A. V. Manohar, *Phys. Lett. B* **255**, 558 (1991).
- [21] J. Engel, M. J. Ramsey-Musolf, and U. van Kolck, *Prog. Part. Nucl. Phys.* **71**, 21 (2013).
- [22] E. E. Jenkins, M. E. Luke, A. V. Manohar, and M. J. Savage, *Phys. Lett. B* **302**, 482 (1993); **388**, 866 (1996).
- [23] U. G. Meissner and S. Steininger, *Nucl. Phys. B* **499**, 349 (1997).
- [24] L. Durand and P. Ha, *Phys. Rev. D* **58**, 013010 (1998).
- [25] S. J. Puglia and M. J. Ramsey-Musolf, *Phys. Rev. D* **62**, 034010 (2000).
- [26] S. J. Puglia, M. J. Ramsey-Musolf, and S. L. Zhu, *Phys. Rev. D* **63**, 034014 (2001).
- [27] B. Guberina and R. D. Peccei, *Nucl. Phys. B* **163**, 289 (1980).
- [28] J. F. Donoghue, X.-G. He, and S. Pakvasa, *Phys. Rev. D* **34**, 833 (1986).
- [29] S. Scherer, *Adv. Nucl. Phys.* **27**, 277 (2003).
- [30] H. Georgi, *Weak Interactions and Modern Particle Theory* (Benjamin/Cummings, Menlo Park, CA, 1984), p. 165.
- [31] J. F. Donoghue, E. Golowich, and B. R. Holstein, *Dynamics of the Standard Model*, Cambridge Monographs on Particle Physics, Nuclear Physics and Cosmology No. 2 (Cambridge University Press, Cambridge, 1992).
- [32] N. Kaiser, P. B. Siegel, and W. Weise, *Nucl. Phys. A* **594**, 325 (1995).
- [33] Y. Hara, *Phys. Rev. Lett.* **12**, 378 (1964).
- [34] A. Le Yaouanc, O. Pene, J. C. Raynal, and L. Oliver, *Nucl. Phys. B* **149**, 321 (1979).
- [35] B. Borasoy and B. R. Holstein, *Phys. Rev. D* **59**, 054019 (1999).
- [36] J. Tandan and G. Valencia, *Phys. Rev. D* **67**, 056001 (2003).
- [37] B. Borasoy and B. R. Holstein, *Phys. Rev. D* **59**, 094025 (1999).
- [38] J. Beringer *et al.* (Particle Data Group), *Phys. Rev. D* **86**, 010001 (2012).

- [39] A. J. Buras and D. Guadagnoli, *Phys. Rev. D* **78**, 033005 (2008).
[40] C. Jarlskog, *Phys. Rev. Lett.* **55**, 1039 (1985).
[41] G. Buchalla, A. J. Buras, and M. K. Harlander, *Nucl. Phys. B* **337**, 313 (1990).
[42] C.-Y. Seng, J. de Vries, E. Mereghetti, H. H. Patel, and M. Ramsey-Musolf, *Phys. Lett. B* **736**, 147 (2004).
[43] R. F. Dashen, E. E. Jenkins, and A. V. Manohar, *Phys. Rev. D* **49**, 4713 (1994); **51**, 2489 (1995).